

Real Time Prediction and Control of Transient Stability Using Transient Energy Function

Pratyasha Bhui, and Nilanjan Senroy, *Member, IEEE*

Abstract-- Real time prediction of transient stability after a fault can potentially prevent occurrence of grid blackouts. In this work, the measurement data obtained from phasor measurement unit (PMU) located at generator buses are used to compute the transient stability margin after a fault has occurred. For evaluating various control actions to be taken to stabilize severely disturbed and unstable generators, the stability margin is estimated using the transient energy function (TEF) technique. A look-up table of various modes of disturbance (MOD) is built offline for different fault locations and post fault topology. Following an actual fault, the most probable MODs are ranked by matching the ‘normalized’ kinetic energy with the look-up table. The correct MOD is then chosen based on the lowest normalized potential energy margin and the Controlling Unstable Equilibrium Point (CUEP) is calculated. This technique overcomes previously reported difficulties in finding the CUEP in real-time applications. With knowledge of pre-fault operating condition obtained from SCADA and the information of the tripped line by analyzing the PMU data, the first swing transient stability margin is computed. The amount of control action needed is subsequently calculated. The proposed method has been tested on the IEEE 39 Bus Test System.

Index Terms-- controlling unstable equilibrium point, transient stability, transient energy function, transient stability control, generation shedding, wide area control.

I. INTRODUCTION

TRANSIENT instability is one of the less probable but most severe events that power systems encounter in daily operation. After a severe disturbance like fault, if proper control action is not taken, then one or more generators may lose synchronism with the rest. Transient instability may cause unintentional islanding, cascaded outages and even wide spread blackouts. Thus, sufficient stability margins must be maintained at every operating point, despite significant economic implications. The ability to predict the transient stability status and assess the severity of a fault in real time may allow the grid to be operated with lower transient stability margins.

Presently available methods for real time prediction of transient stability after a fault, are mostly based on neural networks [1], machine learning methods like decision trees [2]

This work was supported in part by the Department of Science and Technology, Government of India, under its grant DST/RCUK/SEGES/2012/02.

The authors are with the Department of Electrical Engineering, Indian Institute of Technology Delhi, New Delhi, India, and can be reached at pratyasansec@gmail.com, nSenroy@ee.iitd.ac.in.

and support vector machines [3]. In all these methods, faults at different locations of the grid are simulated offline and different dynamic features of power system measurements used to train a classifier to enable it to distinguish between stable and unstable events. These methods were shown to provide acceptable accuracy in classification in a simulation environment. But issues related to the reliability and the practical implementation remain, which are as follows:-

- 1) For a large grid, considering faults of different types, durations and fault impedances at different locations, significant resources are required for generating the data set for training.
- 2) The training data set becomes unreliable with any change in network topology, status of generators and major loads.

- 3) Most of these methods rely entirely on time domain simulations for building the training database which may not provide a quantitative assessment of the fault severity. For instance, in [4] a fixed amount of load shedding was proposed to stabilize the system after an unstable fault irrespective of the fault severity.

Upon successful implementation, the TEF technique has the potential to solve the above mentioned challenges. The central premise of the TEF is that if the energy of the system at the time of fault clearing is higher than the maximum potential energy absorbing capability (i.e. energy at the CUEP), the system will lose synchronism and become unstable [5]. The original problem formulation was relatively unwieldy, and subsequent improvements have been proposed in the calculation of the CUEP [6]-[8]. The kinetic energy of the generators at the fault clearing instant and the deceleration after fault clearing were used to identify the generators which tend to be out-of-step [6]-[7]. These generators, referred to as the *Mode of Disturbance* (MOD), are used to calculate the CUEP. As the method is heuristic in nature, it suffers from convergence problems. A unified method named as *Boundary of Stability Region Based Controlling Unstable Equilibrium Point* (BCU) was introduced to calculate the CUEP [8]. Further research was done to include the detailed generator models [9]-[10], dynamic and structure preserving load models [11], HVDC models [12] etc. The extended equal area criterion was introduced in [13], and it was noted that all the kinetic energy may not contribute to system separation and hence a *corrected* kinetic energy was identified for critical machines [14].

Generator angles were predicted using the accelerating power and generation shedding was proposed to stabilize a

system if instability is detected [15]. The amount of shedding required was estimated using TEF [15-20]. Both the kinetic and potential energy were used as pattern recognition features for dynamic security assessment [21]. The critical trajectory was used to obtain the CUEP from the exit point in BCU method [22]. A transient stability control system was proposed for near real time application in a practical system [23]. Generator models used for simulation as well as energy function calculation, are classical models. However the method is also applicable to 2-axis model with exciter.

Despite several advantages, the real-time applications of TEF remains challenging because of several difficulties, primarily in the calculation of the CUEP [26].

1) The MOD technique suffers from serious convergence problem.

2) The Potential Energy Boundary Surface (PEBS) technique and the BCU method simulate the faulted network to find the exit point on PEBS [27, 8]. Simulating the faulted network to detect the exit point in real time is difficult as knowledge of the fault resistance, type, location etc is needed.

In this work the aim is to predict transient stability after a fault using the PMU data. Both the MOD and the BCU technique have been used to calculate the CUEP. The MOD depends on the distribution of the kinetic energy gained by the generators during fault and the post fault topology. In the offline stage, the MOD is found out for different fault locations in the grid using the BCU. After a fault, the normalized kinetic energy (\bar{KE}) of generators is compared with \bar{KE} calculated offline for different fault locations to identify the most probable MODs. Finally, using the lowest normalized potential energy margin, the correct MOD is identified. Once the MOD is known, the CUEP and the energy margin can be computed to assess the transient stability status and estimate the amount of control action required. To identify the tripped line (post fault topology), sufficient PMUs may be deployed to make the system observable through PMU [28, 29].

The rest of the paper is divided into six sections. Two popular methods of transient stability assessment have been explained in Sec II. Section III presents the proposed method and section IV presents the results obtained. Total computational time and the impact of error in generator angles and speeds have been provided in Sec. V and VI. The advantages of the proposed method have been explained in section VII.

II. TRANSIENT ENERGY FUNCTION

Energy function for power system transient stability studies is well established [5, 14] and used for contingency ranking and other transient stability studies. It describes the total system transient energy for the post disturbance system.

$$V(\omega_i, \theta_i) = V_{KE} + V_{PE} = \{0.5M_{eq}\omega_{eq}^2\} - \{\sum_{i=1}^m P_i(\theta_i - \theta_i^s) + \sum_{i=1}^{m-1} \sum_{j=i+1}^m [C_{ij}(\cos \theta_{ij} - \cos \theta_{ij}^s) + D_{ij} \frac{\theta_i - \theta_i^s + \theta_j - \theta_j^s}{\theta_{ij} - \theta_{ij}^s} (\sin \theta_{ij} - \sin \theta_{ij}^s)]\} \quad (1)$$

where, ω_i =speed of i^{th} generator, M_{eq} = moment of inertia of two machine equivalent, ω_{eq} = speed of two machine equivalent, E =

internal emf, $P_i = P_{mi} - E_i^2 G_{ii}$, θ^s =post fault stable equilibrium point, m=number of generators, $C_{ij} = E_i E_j B_{ij}$, $D_{ij} = E_i E_j G_{ij}$.

The energy function consists of four terms-

- a) $0.5 M_{eq} \omega_{eq}^2$: total corrected kinetic energy of the generators.
- b) $\sum_{i=1}^m P_i(\theta_i - \theta_i^s)$: total potential energy of the generators.
- c) $\sum_{i=1}^{m-1} \sum_{j=i+1}^m C_{ij} (\cos \theta_{ij} - \cos \theta_{ij}^s)$: stored magnetic in all branches
- d) $\sum_{i=1}^{m-1} \sum_{j=i+1}^m D_{ij} \frac{\theta_i - \theta_i^s + \theta_j - \theta_j^s}{\theta_{ij} - \theta_{ij}^s} (\sin \theta_{ij} - \sin \theta_{ij}^s)$: approximate dissipated energy of all branches.

All these energy terms are deviation from steady state values and calculated in COI reference frame. The first term is the kinetic energy and depends on generator speeds only. Last three terms together form the potential energy of the system which depends only on generator angles.

If energy at fault clearing V_{cl} is higher than the maximum potential energy that the post disturbance power system can absorb (this point is called the CUEP, θ^u), then the system will be unstable after fault clearing and vice versa. Therefore the difference of energy at fault clearing (V_{cl}) and the CUEP (V_{cr}) is used as an index to predict transient stability. If ΔV is negative at fault clearing ($\theta_i = \theta_{cl}$), system will become unstable.

$$\Delta V(\omega_i, \theta_i) = \Delta V_{KE} + \Delta V_{PE} = -\{0.5M_{eq}\omega_{eq}^2\} - \sum_{i=1}^m P_i(\theta_i^u - \theta_i) - \sum_{i=1}^{m-1} \sum_{j=i+1}^m [C_{ij}(\cos \theta_{ij}^u - \cos \theta_{ij}) + D_{ij} \frac{\theta_i^u - \theta_i + \theta_j^u - \theta_j}{\theta_{ij}^u - \theta_{ij}} (\sin \theta_{ij}^u - \sin \theta_{ij})] \quad (2)$$

The main focus of research with TEF in past was how to calculate the CUEP. Two significant works on calculation of CUEP has been given below along with the associated difficulties with applying the methods in real time.

A. Mode of Disturbance (MOD) Technique [7,14,30]

After fault clearing, using the kinetic energy gained during the fault and the deceleration of generation after fault clearing, the group of machines tending to lose synchronism are identified. If machines p and q (in an m -machine system) tend to be out of step after fault clearing, MOD = $\{p,q\}$. If the MOD is known, then the corner point (which is very close to the CUEP) can be computed from the post fault stable equilibrium point. Suppose, the vector of rotor angles $[\theta_1^s \theta_2^s \theta_3^s \dots \theta_p^s \dots \theta_q^s \dots \theta_m^s]$ represents the post fault stable equilibrium point (SEP) and the MOD = $\{p,q\}$,

All machines are classified into two groups-

Group I: machines belong to the MOD (Gen p and q here).

Group II: rest of the machines.

$$\theta_I^s = \frac{1}{M_I} \sum_{i \in I} M_i \theta_i^s, \quad \theta_{II}^s = \frac{1}{M_{II}} \sum_{i \in II} M_i \theta_i^s \quad (3)$$

$$\theta_{I-II}^s = \theta_I^s - \theta_{II}^s$$

where, $M_I = \sum_{i \in I} M_i$, $M_{II} = \sum_{i \in II} M_i$

$$\Delta \theta_I = (\pi - 2\theta_{I-II}^s) \left(\frac{M_{II}}{M_I + M_{II}} \right) \quad (4)$$

$$\Delta \theta_{II} = (\pi - 2\theta_{I-II}^s) \left(\frac{M_I}{M_I + M_{II}} \right)$$

$$\theta_I^{u*} = \theta_I^s + \Delta \theta_I, \quad i \in I \quad (5)$$

$$\theta_I^{u*} = \theta_I^s - \Delta \theta_{II}, \quad i \in II$$

Generator angles given by θ_i^{u*} , called corner points are a good estimate of the CUEP in COI reference frame [24]. The exact CUEP θ_i^u may be obtained by solving a optimization problem to minimize $\sum_{i=1}^m |f_i^{PF}(\theta)|$ (eq. 6) on post fault system with θ_i^{u*} as initial choice. The exact CUEP calculated from eq. 6 is used in this work.

The convergence problems of the MOD technique arises from the difficulty to determine the group of machines tending to separate after a fault with absolute certainty. Once the MOD for a fault is known, the CUEP calculation is straightforward.

B. BCU Technique [8]

The convergence problem of the MOD method can be overcome by the BCU method that can calculate the CUEP in a unified manner-

step 1: Obtain post fault SEP by solving $f_i(\theta) = 0$.

$$M_i \frac{d^2\theta_i}{dt^2} = P_i - \sum_{j=1, j \neq i}^n (C_{ij} \sin \theta_{ij} + D_{ij} \cos \theta_{ij}) - \frac{M_i}{M_T} P_{coi} \quad (6)$$

$$= f_i(\theta), \quad i = 1, \dots, m$$

where, $P_i = P_{mi} - E_i^2 G_{ii}$

$$P_{coi} = \sum_{i=1}^m P_i - 2 \sum_{i=1}^m \sum_{j=i+1}^m D_{ij} \cos \theta_{ij} \quad (7)$$

step 2: The faulted network is simulated to obtain the PEBS exit point.

$$M_i \frac{d^2\theta_i}{dt^2} = f_i^F(\theta), \quad i = 1, \dots, m \quad (8)$$

$\sum_{i=1}^m f_i(\theta)(\theta_i - \theta_i^s)$, calculated on post fault network, becomes zero as the system reaches the PEBS boundary. Generator angles at the PEBS is represented as θ^* .

step 3: The gradient system of the post fault system ($\frac{d\theta_i}{dt} = f_i^{PF}(\theta)$) of half the dimensions of the original system (speed dynamics not considered) is integrated until $\sum_{i=1}^m |f_i(\theta)|$ becomes minimum. The exact CUEP is calculated by solving a load flow like minimization problem (step 1) with initial point at the minimum of $\sum_{i=1}^m |f_i(\theta)|$.

BCU method is not suitable for real-time applications as integration of the faulted and the post fault network is time consuming and requires knowledge of the exact fault location, fault resistance etc.

C. Identification MOD using BCU Method in Offline

A fast heuristic method was proposed in [31] along with Extended equal area criterion (EEAC) to identify the MOD. EEAC and Taylor series were used to reduce computational burden by reducing time domain simulation. With high speed of computers of present times, BCU method can be used in offline to get the CUEP that can be used to identify the MOD-

1. BCU method is used in offline to get the CCT of fault at a particular fault location.

2. Time domain simulation is done for a fault duration slightly higher than the CCT.

3. The peak of the potential energy is detected and the generators are ranked in descending order of the angles at that point. As the machines belonging to the MOD have higher angles at that point, the MOD can be identified from the

angles of the generators at that point.

4. Take the top one machine as the MOD, then calculate the CUEP as given in II-A. Calculate the CCT for that fault location with that MOD.

5. Repeat step 4 with top two machine as the MOD, then top three machines and so on. The generator group that gives minimum error between CCT obtained from TEF and time domain simulation can be taken as the MOD.

As the approximate CCT is found out using BCU, calculation of CCT using time domain simulation in offline won't need huge computational burden. After contingency screening, MOD is to be frequently updated for vulnerable fault locations. As MOD depends mostly on fault location and less on operating condition, the look up table of MOD is to be updated less frequently.

In most of the cases BCU method provides the relevant or almost relevant CUEP for a particular fault location. In some critical cases as pointed out in [26], when the machines nearer to the fault don't go out of step, BCU method or its variants fail. However, as BCU method is used for getting approximate CCT only and the exact CCT is found out using time domain simulation, failure of BCU method doesn't affect correct MOD identification in this method.

III. PROPOSED METHOD

The proposed method relies on the fact that PMUs are placed on all the generator buses, and their measurements are available. A look-up table consisting of the MOD and normalized kinetic energy for faults at different locations is initially built from offline simulations. In real-time, the CUEP can be calculated if the MOD is known (Sec-IIIB). Therefore, for an actual fault the normalized kinetic energy of all the machines is compared with the look-up table to rank the possible MODs for that fault. The correct MOD is then identified from the ranked MODs as the one having the minimum normalized potential energy margin $\frac{\Delta V_{PE}}{KE_{corr}}$ (i.e. $\frac{V_{PEcr} - V_{PEcl}}{0.5 M_{eq} \omega_{eq}^2}$) [30] at the instant of fault clearing.

After identifying the correct MOD, the CUEP is calculated as mentioned in Section II-A, and the transient stability margin computed. The entire exercise may be divided into two parts – the offline computation, which has two steps *a*) identification of MOD for different fault locations using BCU method, and *b*) computation of normalized KE gained by the generators for faults at different locations of the grid, and the online computation comprising of three steps – *a*) correct MOD identification after a fault, *b*) assessment of first swing transient stability, and *c*) estimation of the amount of control action required.

A. Offline Computation –building the look-up table

a) MOD identification for different fault location:

For a particular operating condition, the MOD is obtained for different fault locations, as given in Sec-IIIC.

b) Computation of normalized KE gained by the generators:

For fault at a particular location "X" in the grid, the kinetic energy gained by all m -generators in first 0.1s of the fault is

$$KE_X = [ke_{1x} \ ke_{2x} \dots \ ke_{ix} \dots \ ke_{mx}] \quad (9)$$

where ke_{ix} denotes the kinetic energy gained by i -th generator and equals $0.5 M_i \Delta \omega_i^2$, with M_i =moment of inertia and $\Delta \omega_i$ = speed deviation of i^{th} generator. The normalized kinetic energy is the individual generator ke_{ix} divided by total kinetic energy.

$$\begin{aligned} \bar{KE}_X &= [\bar{ke}_{1x} \ \bar{ke}_{2x} \dots \bar{ke}_{ix} \dots \bar{ke}_{mx}] \\ &= \frac{[ke_{1x} \ ke_{2x} \dots \ ke_{ix} \dots \ ke_{mx}]}{\sum_{i=1}^m ke_{ix}} \end{aligned} \quad (10)$$

$$\text{Thus, } \sum_{i=1}^m \bar{ke}_{ix} = 1$$

For a fault at a location "X", if generator i and j go out of step, the MOD is $M = \{i, j\}$. For fault at location "Y", if no generator goes out of step even with sustained fault, $M = \{0\}$.

As MOD may change with large variation in operating condition, \bar{KE} and MOD must be regularly updated for multiple operating conditions on the daily load curve.

B. Online Computation – using PMU data

a) Correct MOD Identification:

After a fault, the correct MOD may be selected from the stored cases as described below.

step 1: Calculation of \bar{KE} - Calculate the \bar{KE} from the generator speeds obtained from the PMU data.

step 2: Ranking of Probable MODs- The MOD depends on the distribution of kinetic energy gained by generators during a fault and as well as the post fault topology. Using k^{th} Nearest Neighbour (k-NN) method [32], the stored fault cases (at all operating conditions) with similar kinetic energy distribution are ranked in ascending order of the Euclidean distance "D" between the stored \bar{KE} calculated for faults at different locations and measured \bar{KE} .

step 3: Calculation of Post-fault SEP- The correct MOD can be chosen using minimum $(\frac{\Delta V_{PE}}{KE_{corr}})$ from the most probable MODs ranked using k-NN method. To do so, the post fault SEP and the CUEP for each of the ranked MODs are calculated. Considering the tripped line is known if the system is PMU observable or following the method proposed in [28], the post fault SEP (θ^s) can be calculated (step 1, Sec II-B).

step 4: Calculation of CUEP- For each ranked MOD, the CUEP is calculated as explained in Sec II-A. (Eq. 5 & 6).

step 5: Identification of the Correct MOD- Among all the MODs ranked, the first few are tested to identify the correct MOD. The lowest normalized potential energy margin $(\frac{\Delta V_{PE}}{KE_{corr}})$ identifies the correct MOD where, ΔV_{pe} is the difference between potential energy at fault clearing instant and at the CUEP. The KE_{corr} is the corrected kinetic energy of two machine equivalent of the system at fault clearing instant [14].

b) Assessment of first swing transient stability:

Calculate the energy margin of the system at the instant of fault clearing ($\Delta V_{cl} = V_{cr} - V_{cl}$). If the energy of the system at fault clearing instant (V_{cl}) is less than the energy at the CUEP (V_{cr}), then ΔV_{cl} is positive and system will remain stable and vice versa.

c) Estimation of the Amount of Control Actions Required and Monitoring of Stability Status:

Prediction of generator speed and angles: If generation shedding is required to stabilize the system after a fault, the speed of the generators at the instant of shedding has to be predicted. The minimum amount of data available for this prediction corresponds to the computational delay associated with the application of the TEF technique (say $T_1 \sim 0.05$ s). For practical implementation with online WAMS data, there are other delays associated signal latency ($T_d \sim 0.025 - 0.1$ s) and initiating control actions ($T_c \sim 0.05$ s). Therefore, data of duration at least T_1 s after the fault clearing has to be used to predict the generators' speeds and angles $(2T_d + T_c + T_1)$ s after fault clearing. The prediction function must be selected to ensure optimal performance with minimum data.

For the purpose of testing various prediction functions, data from a 0.05 s and 0.1 s time window were tested for prediction. The error in predicting generator angles after $(2T_d + T_c + T_1)$ time is shown in TableI. Combining the Quadratic fit and the Cubic fit yielded the best result with low average error in predicting generator angles and speeds, much below the permissible error in predicting angles which was taken as 10° in [16]. Fast simulation methods can be used instead of curve fitting which will result in lesser error.

TABLE I: AVERAGE ERROR IN PREDICTED GENERATOR ANGLES FOR DIFFERENT PREDICTION FUNCTIONS

Prediction Function	Duration of data used for prediction (s)	Instant at which data is to be predicted (s)	Average Prediction Error (Degree)
Quadratic	0-0.05 s	0.2	11
		0.25	21
		0.3	35
	0-0.1 s	0.25	11.9
		0.3	20.9
		0.35	30
Cubic	0-0.05 s	0.2	3.05
		0.25	9
		0.3	21
	0-0.1 s	0.25	6.7
		0.3	16.4
		0.35	29.4
(Quadratic fit + Cubic fit)/2	0-0.05 s	0.2	2.55
		0.25	7
		0.3	9.8
	0-0.1 s	0.25	3.2
		0.3	4.3
		0.35	6.3
Fast Generation Shedding Equipment [15]	0-0.05 s	0.2	23
		0.25	28
		0.3	35

Modification in Energy Function for Generation Shedding: If generation shedding is assumed in a plant the generator inertia, input power, and transient reactance are to be changed while calculating energy margin. If P_{sh} power (pu value) is shed from i^{th} generator, then the new values are,

$$H_{new} = H(1 - P_{sh})$$

$$P_{new} = P(1 - P_{sh})$$

$$X'_{dnew} = \frac{X_d}{1 - P_{sh}}$$

Estimation of the amount of control actions required: A flowchart to estimate the control action required to stabilize the system is shown in Fig. 1. The selection of the plant for

generation shedding is done offline on the basis of maximum sensitivity of the energy margin to generation shedding [24] in different plants. The energy margin is calculated for different amounts of shedding as shown in Fig. 1.

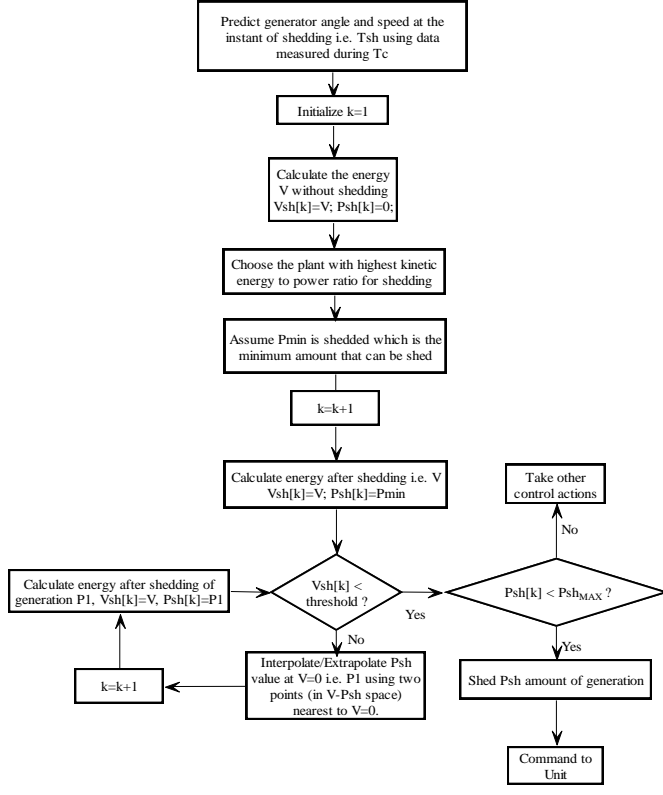


Fig. 1: Flowchart for generation shedding

After completion of the control action, the energy margin ($V(t) - V_{cr}$) is re-calculated. If it is unstable, further control action is required. In case very high amounts of generation are required to be shed to stabilize the system, there may be alternative emergency control strategies such as controlled islanding that may be more appropriate.

IV. RESULT

As the MOD of a particular fault location may change with operating condition, both MOD and \bar{KE} are calculated for two different operating conditions (say at 10:00 AM and 10:30 AM). The method was tested on the IEEE 39 bus test system [25] shown in Fig. 2. Operating condition one is the actual data given in [25] wherein second operating condition was obtained by adding a load of 400 MW at bus 22 and supported by generator 7. This is just to show how the method works, otherwise all the loads may vary with time in real system. The fault is considered to occur between 10:00-10:30 AM.

There are total fifteen MODs in the system for the two operating conditions, as given in Table II with corresponding fault locations. For example, for a fault on Line 1-2, the MOD is $M1 = \{1, 2, 3, 4, 5, 6, 7, 8, 9\}$, and for a fault at bus 16, the MOD is $M2 = \{3, 4, 5, 6, 7, 8, 9\}$. For line faults, a single circuit line was replaced with a double circuit line of same equivalent impedance and the fault was cleared by removing the faulted circuit. Source impedance in generators were taken as sub-transient impedances, as recommended by PSS/E.

For every fault location, MOD is identified and the \bar{KE} calculated offline for two operating conditions and stored. It may be noted that for changes in fault location and post-fault topology, the MODs may or may not change, but the \bar{KE} must always change. MODs and \bar{KE} for two fault locations and operating conditions have been given in Table III.

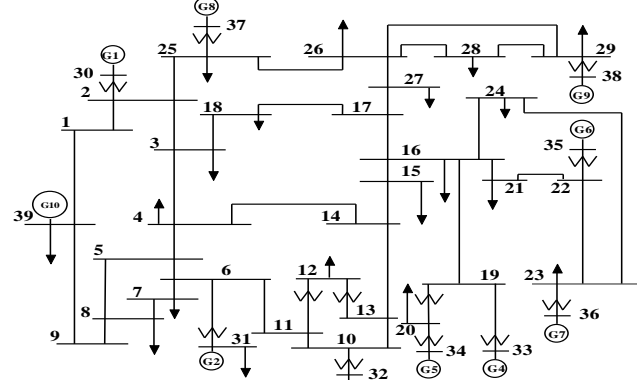
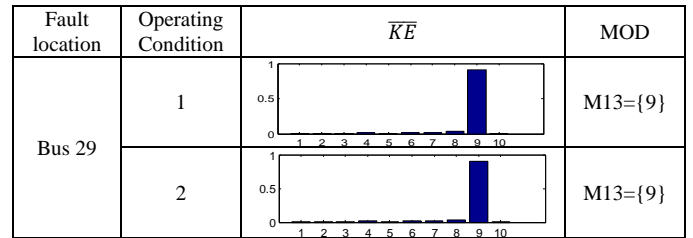


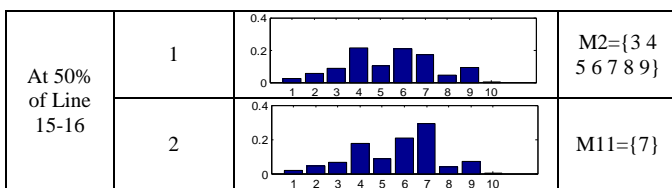
Fig. 2: IEEE 39 bus test system

TABLE II: MODS AND CORRESPONDING FAULT LOCATIONS

MOD	Fault Locations	
	Operating Condition 1	Operating Condition 2
$M1=\{1, 2, 3, 4, 5, 6, 7, 8, 9\}$	Line: 1-2, 2-3	Line: 1-2, 2-3
$M2=\{3, 4, 5, 6, 7, 8, 9\}$	Bus: 2, 16, 17, 18, 21, 24, 25, 30 Line: 3-18, 15-16, 17-18	Bus: 2, 16, 17, 18, 21, 24, 25, 30 Line: 3-18, 17-18, 17-27
$M3=\{2, 3, 4, 5, 6, 7, 9\}$	Bus: 1, 3, 4, 5, 6, 7, 8, 9, 10, 11, 12, 13, 14, 15, 39 Line: 3-4, 4-5, 4-14, 5-6, 5-8, 6-7, 6-11, 7-8, 8-9, 10-13, 13-14, 14-15, 16-17, 17-27, 10-11	Bus: 1, 3, 4, 5, 6, 7, 8, 9, 10, 11, 12, 13, 14, 15, 39 Line: 3-4, 4-5, 4-14, 5-6, 5-8, 6-7, 6-11, 7-8, 8-9, 10-13, 13-14, 14-15, 10-11
$M4=\{4, 5, 6, 7\}$	Line: 16-19, 16-24	Line: 16-19
$M5=\{4, 5\}$	Bus: 19, 33	Bus: 19, 33
$M6=\{6, 7\}$	Bus: 22, 23, 35	Bus: 22, 23, 35
$M7=\{1, 8, 9\}$	Line: 2-25	Line: 2-25
$M8=\{\text{null}\}$	Line: 1-39, 9-39	Line: 1-39, 9-39
$M9=\{3\}$	Bus: 32	Bus: 32
$M10=\{5\}$	Bus: 20, 34	Bus: 20, 34
$M11=\{7\}$	Bus: 36	Bus: 36 Line: 23-24, 22-23, 21-22, 16-24, 16-21, 16-17, 15-16
$M12=\{8\}$	Bus: 37	Bus: 37
$M13=\{9\}$	Bus: 26, 27, 28, 29, 38 Line: 25-26, 26-27, 26-28, 26-29, 28-29	Bus: 26, 27, 28, 29, 38 Line: 25-26, 26-27, 26-28, 26-29, 28-29
$M14=\{4, 5, 6, 7\}$	Line: 16-21, 21-22, 23-24	
$M15=\{2\}$	Bus: 31	Bus: 31

TABLE III: \bar{KE} AND MOD FOR DIFFERENT FAULT LOCATIONS, CALCULATED OFFLINE USING SIMULATION DATA





With the offline look-up table built as described before, the proposed method has been shown with three test cases where WAMS data have been used for transient stability control.

A. Fault on bus 29, MOD is M13 = {9}

Offline Computation:

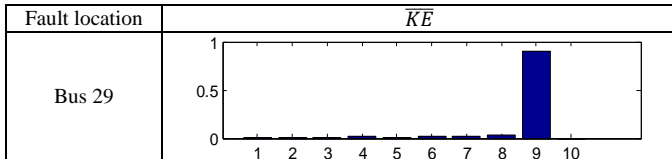
MODs and \bar{KE} for faults at different buses and lines are calculated offline and stored for two operating conditions along the daily load curve as explained before.

Online Computation:

If a fault occurs in the period between the two operating points, for which MODs were identified and stored, the correct MOD will be identified from the stored ones. Therefore, the method has to be tested for a new operating condition, that lies in between the two. Load at bus 22 was taken as 200 MW and this is considered to be the third operating condition.

step 1: Calculation of \bar{KE} : A balanced fault of duration 0.18s was created at bus 29. The \bar{KE} gained by the generators in first 0.1s of the fault was calculated from the speeds measured by PMU which has been shown in Table IV.

TABLE IV: \bar{KE} GAINED BY GENERATORS IN 0.1 s OF FAULT AT BUS 29,
CALCULATED USING SPEEDS MEASURED WITH PMU



step 2: Ranking of Probable MODs- Using k-NN method, the MODs for fault cases similar to the actual fault, were detected and then ranked in ascending order of the Euclidean distance "D" from \bar{KE} measured to \bar{KE} stored offline. First few ranked MODs are shown in Table V.

After M13, the next closer MODs are M3, M7, M2 etc.

step 3: Calculation of the Post Fault SEP- The post fault stable equilibrium point was calculated as per Step 1 of Sec. II-B.

$$\theta^s = [-0.024 \ 0.204 \ 0.3033 \ 0.254 \ 0.38 \ 0.286 \ 0.55 \ 0.249 \ 0.46 - 0.1591]$$

step 4: Calculation of the CUEP for Each MOD- For each MOD, corresponding CUEP was calculated as per Sec. II-A (eq. 5 & 6). For example, the CUEP for MOD M13 is-

$$\theta^u = [0.116 \ 0.317 \ 0.475 \ 0.549 \ 0.667 \ 0.593 \ 0.88 \ 0.52 \ 2.372 \ 0.0406]$$

step 5: Identification of the Correct MOD- For each MOD, the $(\frac{\Delta V_{PE}}{KE_{corr}})$ was calculated at the time of fault clearing. Minimum of $(\frac{\Delta V_{PE}}{KE_{corr}})$ indicates the correct MOD. Table VI shows that the correct MOD for a fault on bus 29 is M13 = {9}.

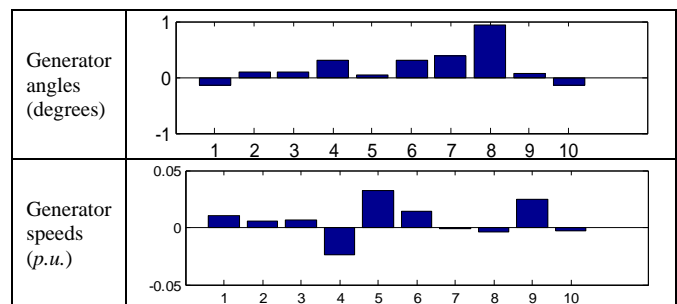
Table VI: Identification of the Correct MOD from the Ranked MODs

MOD	M13	M3	M7	M2
$\frac{\Delta V_{PE}}{KE_{corr}}$	0.8458	8.852	4.323	7.56

step 6: Assessment of first swing transient stability: Use the CUEP calculated in step 4 for MOD 13, to calculate the energy at fault clearing and the CUEP. In this case, V_{cl} is 4.979 and V_{cr} comes out to be 4.24. As $V_{cl} > V_{cr}$, the system will become unstable.

step 7: Prediction of Generator Angles and Speeds- As explained in Section III-B, generator angles and speeds have to be predicted at the instant of shedding using 0.05 s data after fault clearing. This instant is taken approximately as 0.2s after fault clearing. The error between the predicted and actual values of angle and speed after 0.2s of fault clearing is shown in Table VII and found to be very less for all ten generators.

TABLE VII: ERROR BETWEEN PREDICTED AND ACTUAL VALUES



step 8: Estimation of Control Action Required- If energy margin is known, control actions can be taken like generation shedding (amount and location), dynamic braking (resistance value, location and duration of on time), fast valving (location, duration and percentage of opening) etc. In this work, generation shedding has been used as transient stability control.

Generation was shed from plant 9 after 0.2 s of fault clearing. The amount of shedding required to stabilize the system was calculated from TEF which was further verified using time domain simulations (TDS) as given in Table VIII.

TABLE VIII: AMOUNT OF GENERATION SHEDDING REQUIRED

Fault Duration (s) (CCT=0.173)	Amount of Shedding Required (in percentage of 9 th generator output)	
	TEF	TDS
0.174	11%	1%
0.180	32%	22%
0.184	49%	40%

It can be seen that TEF provides result with sufficient accuracy. Though CCT for fault at bus 29 is 0.173s, TEF gives CCT as 0.164s that causes an inherent error in calculating control actions required. If the fault duration is in between 0.164 s and 0.173 s, TEF will show the system as unstable though the system is actually stable. It may be noted that generation shedding is done by tripping single or multiple units. Therefore error of few percentage is acceptable. Dynamic braking and other lighter control actions may be used when TEF shows the system as marginally unstable.

TABLE V: RANKING OF THE MODS IN ASCENDING ORDER OF EUCLIDEAN DISTANCE "D"

D	0.0103	0.0109	0.0149	0.0328	0.0358	0.0483	0.0566	0.0603	0.11	0.651	0.669	0.693	0.7	0.725
Fault location	Bus 29	Bus 29	Line 28-29	Line 28-29	Bus 28	Bus 38	Bus 28	Bus 38	Line 26-29	Line 17-27	Line 2-25	Line 2-25	Line 17-27	Bus 2

Operating condition	1	2	1	2	1	2	2	1	1		1	1	2	2	2	1
MOD	M13		M3	M7	M7	M2	M2									

B. Fault on bus 15: MOD is M3 = {2, 3, 4, 5, 6, 7, 9}

This is an example of inter area mode separation after a fault. Generator 10 has very high inertia as it is the aggregated model of a group of generators. Generator 1 and 8 are strongly coupled with the 10th generator. Therefore, after a fault at bus 15, rest of the generators tends to be out of step. Fault duration was taken as 0.287s while the CCT computed using time domain simulation was 0.267s.

I. Offline Computation:

It is similar to the previous case.

II. Online Computation:

Loads are assumed to be the same as given in Sec. IV-A.

Steps1-4 can be done similar to the Sec. IV-A.

step 5: Identification of Correct MOD- For each MOD, $(\frac{\Delta V_{PE}}{KE_{corr}})$ is calculated after fault clearing. Minimum of $(\frac{\Delta V_{PE}}{KE_{corr}})$ indicates the correct MOD. Table IX shows that the correct MOD is M3 = {2, 3, 4, 5, 6, 7, 9}.

TABLE IX: IDENTIFICATION OF THE CORRECT MOD FROM THE RANKED MODS

MOD	M3	M2	M11	M5	M13
$\frac{dV_{pe}}{KE_{corr}}$	0.995	1.05	1.52	2.6	3.16

step 6: Assessment of first swing transient stability: Use the CUEP calculated in step 4, to calculate the energy at the instant of fault clearing and the CUEP. V_{cl} is 12.47 and V_{cr} comes out to be 11.65. As $V_{cl} > V_{cr}$, the system will become unstable.

step 7: Prediction of Generator Angles and Speeds- Generator angles and speeds were predicted at the instant of generation shedding i.e. 0.2 s after fault clearing.

step 8: Estimation of Control Action Required- Generation was shed from plant 7 as it was showing highest sensitivity of energy margin to shedding and hence less amount generation would be required. Amount of generation shedding required as obtained using the proposed TEF technique was 55% which is very close to the shedding required obtained from TDS that comes out to be 50%.

C. Fault at 50% of line 1-39: MOD={null}

This is a very rare case of no separation even after sustained fault. Kinetic energy gained by the generators during fault is such that all the generators accelerate together.

Offline Computation:

It is similar to the previous case presented in Sec. IV-A.

Online Computation:

Loads are assumed to be the same as given in Sec. IV-A. Steps1-3 can be done similar to the Sec. IV-A.

step 4: Calculation of the CUEP for Each MOD- CUEP is calculated for all MOD except MOD={0}.

step 5: For first few MODs ranked in ascending order of the distance "D", The $(\frac{\Delta V_{PE}}{KE_{corr}})$ was calculated at the time of fault clearing. If no generator is going to be out of step, KE_{corr}

would be zero. Therefore, the $(\frac{\Delta V_{PE}}{KE_{corr}})$ was not calculated for MOD = {null}. The minimum of $(\frac{\Delta V_{PE}}{KE_{corr}})$ in Table X indicates the correct MOD which is M_i={1, 2, 3, 4, 5, 6, 7, 8, 9}.

TABLE X: IDENTIFICATION OF THE CORRECT MOD

MOD	M8	M1	M3	M7	M2
dV_{pe}/KE_{corr}	-	47.8076	65.896	169.748	59.846

step 6: Use the CUEP calculated in step 4 for MOD M1, to calculate the energy at the fault clearing instant and the CUEP. $\theta^u = [1.07 \ 1.677 \ 1.824 \ 1.716 \ 1.831 \ 1.772 \ 2.083 \ 1.479 \ 1.88 - 0.95]$ V_{cl} is 0.2695 and V_{cr} comes out to be 14.995. As $V_{cl} < V_{cr}$, the system will remain stable and no control action is required.

D. Other Faults:

The method was tested for faults at different buses and on different lines. Results are given in Table XI. For line faults, one circuit was tripped out of the two while no line was tripped for bus faults.

TABLE XI: ESTIMATION OF THE GENERATION SHEDDING REQUIRED FOR FAULTS AT DIFFERENT LOCATIONS

Fault Location	CCT (s) TEF,TDS	Fault duration	MOD	Generation shedding required in percentage of the output of shedded generator		
				Gen No	TEF	TDS
Line 2-3	0.421, 0.417	0.43	M1	7	23%	29%
Bus 2	0.317, 0.319	0.33	M2	7	26%	28%
Line 16-19	0.27, 276	0.29	M4	7	27%	20%
L10-11	0.319, 0.312	0.32	M3	7	32%	37%
L6-11	0.33, 0.332	0.34	M3	7	40%	32%
36	0.165, 0.18	0.19	M11	7	100%	85%
34	0.26, 0.265	0.28	M10	5	100%	100%
37	0.277, 0.283	0.29	M12	8	100%	100%

E. Demonstration using Time Domain Simulation

The method has been demonstrated for the first fault case (described in Sec. IV-A) using time domain simulation in Fig. 3. It can be seen that without control action the system becomes unstable after fault clearing whereas the system remains stable after 49% generation shedding at 9th generator. In practice, generation shedding is to be done not by certain percentage, but single or multiple units is to be tripped.

It may be noted that TEF is not as accurate as time domain simulation. If the fault duration is in between 0.164s (CCT obtained from TEF) and 0.173s (CCT obtained from TDS), TEF will show the system as unstable though the system is actually stable. But the energy margin (represents fault severity) obtained from TEF will show a smaller value and hence a small amount of generation shedding required, which may be . The biggest advantage of using TEF is that it can give indication of fault severity, depending on which amount and type of control action can be decided.

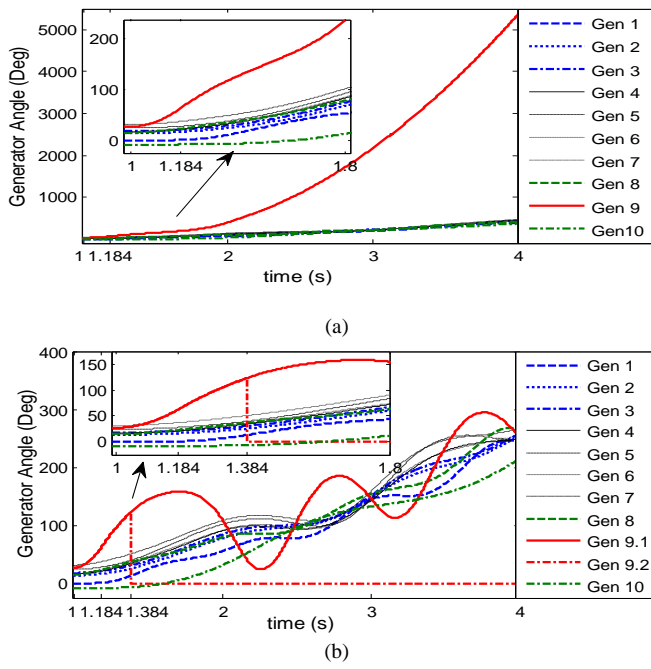


Fig.3: Fault occurs at bus 29 at 1s, cleared at 1.184s. a) no control action, system instability b) 49% generation shed at 9th Gen at 1.384 s, stable case.

F. Performance on Northern Grid of India

The method was also tested on Northern Grid of India having 57 machine, 246 bus and 372 line test system Plant 40 and 42 in the original system were kept offline. A three phase fault was applied at bus 157 at 1s and cleared after 1.39s. CCT for the bus was 0.38s.

Offline Computation:

It is similar to the previous case presented in Sec. IV.

Online Computation:

Steps 1-4 can be done similar to the Sec. IV-A.

step 5: Identification of the Correct MOD- For the top MODs ranked using *knn-search* method, the $(\frac{\Delta V_{PE}}{KE_{corr}})$ was calculated at the time of fault clearing. Minimum of $(\frac{\Delta V_{PE}}{KE_{corr}})$ indicates the correct MOD.

TABLE XII: IDENTIFICATION OF THE CORRECT MOD FROM THE RANKED MODS

MOD	{31 32}	{null}	{40}	{20 21 25}
Fault location	Bus 157	Bus 177	Bus 30	Bus 18
$\frac{\Delta V_{PE}}{KE_{corr}}$	0.8974	-	9632	1001

Table XII shows that the correct MOD for a fault on bus 157 is {31 32}. The magnitude of $(\frac{\Delta V_{PE}}{KE_{corr}})$ is very high for the last two MOD as KE_{corr} is very less for these MODs. Second ranked MOD is {null}, i.e. no generator becomes out of step even after a long duration fault. As there is no generator in the MOD, $\frac{\Delta V_{PE}}{KE_{corr}}$ is not calculated for that MOD.

step 6: Assessment of first swing transient stability: Use the CUEP calculated in step 4, to calculate the energy margin at the instant of fault clearing and the CUEP. As $(V_{cr} - V_{cl})$ is negative (-0.7351), the system will become unstable.

step 7: Prediction of Generator Angles and Speeds- Generator angles and speeds were predicted at the instant of generation shedding i.e. 0.2 s after fault clearing.

step 8: Estimation of Control Action Required- Generation was shed from generator 31 (bus 21) as it was having highest sensitivity of energy margin to generation shedding. The amount of generation shedding required as obtained using the proposed TEF technique was 95%. It was verified using repeated time domain simulations (TDS) with different amount of generation shedding that comes out to be 100% which is very close to the result obtained from TEF.

Generator angles are shown with and without generation shedding in Fig. 4. It may be noted that TEF provides amount of shedding slightly less than the actual amount of shedding obtained from time domain simulation. Therefore, if 95% of generation is shedded from generator 31, it will not be able to stabilize the system. However part of a generator can't be shed practically. In practice, generation will be shedded in multiple of units, hence generator 31 is to be tripped. Thus, the TEF method is clearly able to estimate the severity of the fault.

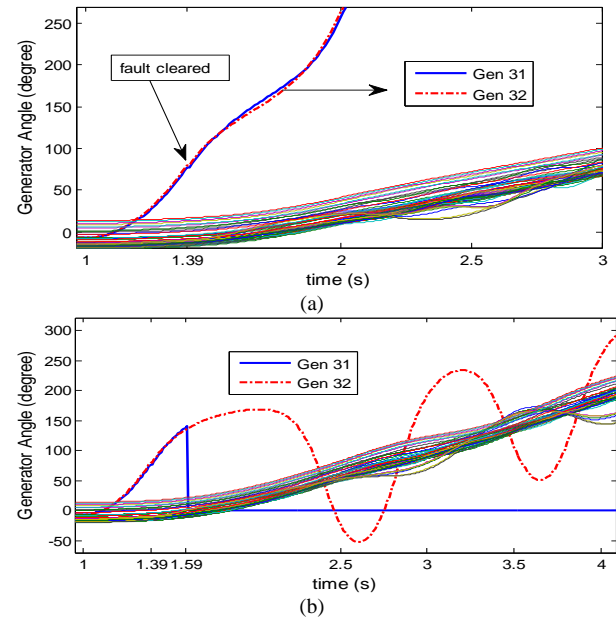


Fig.4: Fault occurs at bus 157 at 1s, cleared at 1.39s. a)no control action, generator 31 (bus 21) and 32 (bus 22) become out of step initially. b)Generator 31 is tripped at 1.59s, system remains stable.

V. COMPUTATION TIME

All the programs were run in MATLAB 2010a using DELL i7, 3.1 GHz, 8GB RAM system. The computation time of each step in the proposed strategy is given in Table XIII.

TABLE XIII: COMPUTATION TIME OF EACH STEP OF THE METHOD

Computation Steps	Computation Time (s)
A. Offline Computation	
1.Post fault SEP	0.002
2. Calculation of CUEP using BCU	0.08+0.051+0.04 +0.03+0.002
3. Simulation with fault duration slightly greater than the CCT	0.089
4. Rank machines in descending order of angles at the peak of potential energy	0.0001
5. Add machines to the MOD from the top in the ranking, Compute the CCT for each case	(0.0005+0.006)*(m-1)

6. Identify the correct MOD having minimum error between CCTs obtained for different MODs and time domain simulation	0.00001
Total Computation Time for each fault location	0.3526
B. Online Computation	
1. Formation of Reduced Y-bus	0.001
2. Calculation of KE and Ranking of MODs	0.002
3. Post-fault SEP	0.0005
4. Calculation of CUEP for each MOD	0.0005
5. Calculation of $\left(\frac{\Delta V_{PE}}{KE_{corr}}\right)$ for each MOD, Identification of Correct MOD	0.0003
6. Stability Prediction	0.0003
7. Prediction of Angle/ Speed at the instant of Control Action for each generator (Time domain simulation for 0.2s takes 0.005s)	0.00124
7. Calculation of ΔV (stability status) for each value of shedding ΔP .	(0.001+0.0005 +0.0003)
Total Computation Time	0.0076

Comments- 1. The BCU computation time includes *a*) fault simulation for 0.5s using PSS/E Ver. 33, *b*) PEBS boundary detection, *c*) simulation of gradient system for angle dynamics only, detection of minimum of $\sum_{i=1}^m |f_i(\theta)|$ (Sec II-B), *d*) computation of CUEP. The pre-fault SEP computation time is not included as it is calculated only once, while the other steps have to be carried out for different faults locations.

2. Offline calculation of post fault SEP and CUEP part are done in 3-4 Newton-Raphson iterations, using reduced Jacobean, as only active power balance equations are used and voltage of load buses are absent (generator internal emf is taken constant). Online, as the post-fault SEP is expected to be close to the pre-fault SEP, a single iteration is usually enough.

3. Step B.4 and B.5 in Table 12 are to be computed for different MODs in parallel. The computation time is given for one MOD in the Table 12.

4. Step B.6, The computation time for predicting the angle of one generator using curve fitting is given. For multiple generators, it can be computed in parallel. Interestingly, time domain simulation of the post fault system to get the angles and speed after 0.2s of fault clearing (~at the instant of control action) requires only 0.005s with constant admittance load model for a 10 machine 39 bus system in PSS/E. It is quite less and therefore can be used instead of curve fitting.

5. Step B.7 in Table 12 includes new Y-bus formation due to change in X'_d , CUEP (old CUEP as initial choice) and ΔV after shedding. In this case, computation of SEP is not required to find the new CUEP.

6. Instead of calculating reduced Y-bus multiple times from scratch (topology change after fault, change in X'_d after shedding), old Y_{bus} can be modified to get the new values [33].

6. All the computations were done in Matlab 2010a except time domain simulations which were done using PSS/E 33. With more efficient supercomputers, the computation time is expected to be even smaller. The total online computation time is considerably less keeping a safe margin for any extra time delay during practical implementation.

VI. IMPACT OF ERROR IN GENERATOR SPEED AND ANGLE

Generally generator speeds are measured from the rotor shaft. However there may be error in measurement, especially if these quantities are estimated from terminal measurements using dynamic state estimation. There may also be error in predicting generator angles and speeds at the instant of shedding if instability is predicted. The impact of error in generator angles and speeds can be physically understood from sensitivity of energy margin with respect to the errors.

A. Impact of Error in Speed of i^{th} Generator- Speed of a generator effects only the kinetic energy part of the energy margin (ΔV). Sensitivity of ΔV to the speed of i^{th} generator is

$$\begin{aligned}\frac{\partial(\Delta V)}{\partial \omega_i} &= 0.5 M_{eq} \omega_{eq} \left(\frac{M_i}{M_{MOD}} \right), i \in MOD, \\ &= 0.5 M_{eq} \omega_{eq} \left(-\frac{M_i}{M_{rest}} \right), i \in rest \text{ of the generators}\end{aligned}$$

$$\text{where, } M_{MOD} = \sum_{i \in MOD} M_i, M_{rest} = \sum_{i \in rest} M_i$$

Sensitivity of energy margin with respect to speed of i^{th} generator

(a) is high when the equivalent speed, ω_{eq} , between generators belonging to MOD and remaining generators is high

(b) is high when ratio of inertia of i^{th} generator and the total inertia of that group (MOD or rest of the generators) is high.

(c) is positive if the generator belongs to MOD and vice versa. It means with positive error, it will increase the energy margin if the generator belongs to MOD and vice versa.

The maximum and minimum error in energy margin can be found out for a given error margin in generator speeds. Error in energy margin at the fault clearing instant will affect the stability prediction, and error in ΔV at the instant of control action will affect the estimation of generation shedding required. The error in energy margin for different levels of error in generator speeds is shown in Table XIV. Error in energy margin consists of error in kinetic energy and error in potential energy (which is zero as it is independent of speed). Fault on bus 2 has been considered (MOD=[3 4 5 6 7 8 9], see table 11). As per (a) above, error is lesser at the instant shedding as equivalent speed ω_{eq} is also lesser at that instant. However as the magnitude of KE_{corr} is much lesser, net error becomes high in percentage at the instant of shedding.

TABLE XIV: ERROR IN KE_{corr} FOR DIFFERENT ERROR IN GENERATOR SPEED

Error in Speed (percentage)	Error in Kinetic Energy (percentage), Error in Potential Energy is zero			
	At fault clearing instant		At the instant of shedding	
	Max	Min	Max	Min
0.5%	1.26%	-1.25%	2.23%	-2.20%
1%	2.52%	-2.50%	4.48%	-4.38%
1.5%	3.80%	-3.73%	6.76%	-6.54%
2%	5.08%	-4.96%	9.06%	-8.67%
2.5%	6.38%	-6.18%	11.4%	-10.8%

B. Impact of Error in Angle of i^{th} Generator- Angle of a generator effects only the potential energy of the energy margin (ΔV). Sensitivity of ΔV_{PE} with respect to generator angle can be found out, however kinetic energy, it's difficult to visualise the error in potential energy from analytical expression for random error in generator angle. Random error was added to the measured angles (at fault clearing instant for

stability prediction) and predicted angles (at the instant of control action). The error in energy margin (average of 20 ensemble) for different level of random error in angles is given in Table XV.

TABLE XV: ERROR IN ΔV_{PE} FOR DIFFERENT ERROR IN GENERATOR ANGLE

Random Error in Angle (deg)	Error in Potential Energy Margin (percentage)	
	At fault clearing instant	At the instant of shedding
-1 to +1	1.34%	3.11%
-2 to +2	1.78%	5.76%
-3 to +3	3.11%	7.55%
-4 to +4	4.63%	11.2%
-5 to +5	6.71%	14.1%

VII. ADVANTAGES OF TEF

Till date, TEF has not been applied in the context of real-time security assessment and control. However, using the strategy proposed in this paper, TEF may be adapted to online transient stability assessment and alleviation. Some of the advantages of the original TEF method of particular interest in real-time applications are as follows:

1. In conventional TEF technique, the CUEP calculation required simulation of the faulted and post-fault system which may not be feasible in real-time application. In this paper, this task is accomplished by identifying the correct MOD using the normalised potential energy margin.

2. In this technique, the MOD is to be calculated only once for a particular fault location, unlike other machine learning techniques, wherein for a particular fault location, simulations are required for different fault durations, resistances and types.

3. In the context of offline data-set generation, if the system topology changes, the data set generated for machine learning techniques, has to be regenerated. Whereas for the TEF method, the fault cases most affected by topology changes, may be identified from sensitivity techniques [33]. Therefore, only few fault cases may need to be regenerated.

4. As the MOD depends mostly on fault location and less on operating condition, the look up table is to be updated less frequently.

5. Machine learning techniques use training data in which all detailed calculations are done offline for very few operating condition, fault durations and locations. Therefore the effect of all these factors can't be accurately included in control actions. Some of the transient stability control techniques predict stability by comparing the angle difference with the biggest generator [15, 17]. However, the biggest generator itself may become out of step, or kept offline. As detailed stability calculations are done online, the effect of fault duration, type, resistance etc are taken into account in the proposed method.

Future Work - Inclusion of Detailed Model: In this work, classical models have been used for both simulation and energy function. However, as the MOD technique is valid for both classical and detailed models [24,35], the method can be extended for detailed model also. Among all the controls, only exciter impacts first swing transient stability significantly. Inclusion of exciters in this method is given below-
Energy function for detailed generator model is given below-

$$V(\omega_i, \theta_i) = 0.5M_{eq}\omega_{eq}^2 - \sum_{i=1}^m (P_{mi} - \alpha_{ii}G_{ii})(\theta_i - \theta_i^*) + \sum_{i=1}^{m-1} \sum_{j=i+1}^m [B_{ij}\alpha_{ij}(-\cos\theta_{ij} + \cos\theta_{ij}^*) + B_{ij}\beta_{ij}(\sin\theta_{ij} - \sin\theta_{ij}^*) + G_{ij}\alpha_{ij}\frac{\theta_i - \theta_i^* + \theta_j - \theta_j^*}{\theta_{ij} - \theta_{ij}^*}(\sin\theta_{ij} - \sin\theta_{ij}^*) + G_{ij}\beta_{ij}\frac{\theta_i - \theta_i^* + \theta_j - \theta_j^*}{\theta_{ij} - \theta_{ij}^*}(\cos\theta_{ij} - \cos\theta_{ij}^*)]$$

$\alpha_{ij} = E'_{di}E'_{dj} + E'_{qi}E'_{qj}$, $\beta_{ij} = E'_{di}E'_{qj} - E'_{qi}E'_{dj}$, G, B are real and imaginary part of the reduced admittance matrix.

Exciter effect on E'_{di} and E'_{qi}

Though E'_{di} and E'_{qi} continuously change after fault clearing, their values can be taken as constants (average of the values at the fault clearing and the peak point).

$$E'_{di} = 0.5(E'_{di,clearing} + E'_{di,peak}), E'_{qi} = 0.5(E'_{qi,clearing} + E'_{qi,peak})$$

Values of the E'_{di} and E'_{qi} at the peak of a critically stable trajectory can be calculated using a simpler exciter model as given in [35], or from a time domain simulation of a critically cleared fault. As E'_{di} and E'_{qi} at the peak is not dependent on fault duration like the CUEP [35], it can be calculated offline for different fault locations and stored in a look-up table similar to the normalized kinetic energy in the proposed method.

Computational burden- Suppose

$$X1 = (-\cos\theta_{ij} + \cos\theta_{ij}^*), X2 = (\sin\theta_{ij} - \sin\theta_{ij}^*), X3 = \frac{\theta_i + \theta_j - \theta_{ij}^* - \theta_{ij}}{\theta_{ij} - \theta_{ij}^*}$$

Then energy function becomes-

$$V(\omega_i, \theta_i) = 0.5M_{eq}\omega_{eq}^2 - \sum_{i=1}^m (P_{mi} - \alpha_{ii}G_{ii})(\theta_i - \theta_i^*) + \sum_{i=1}^{m-1} \sum_{j=i+1}^m [B_{ij}\alpha_{ij}X_1 + B_{ij}\beta_{ij}X_2 + G_{ij}\alpha_{ij}X_3X_2 + G_{ij}\beta_{ij}X_3(-X_1)]$$

As the calculations in equation (12) above are simple arithmetic, computational burden depends mostly on the number of inner loops (Number of generators in this case) which remains same. As (X1, X2, X3) are also calculated for classical model, computational burden in the online part of this method remains almost same in classical and detailed model.

Accuracy- The proposed method was tested for detailed models (PSS data taken from [36], no exciter for Gen 10). From table XVI, it can be said that the method with detailed model is sufficiently accurate. Accuracy of TEF with average E'_{di} and E'_{qi} was also tested in [35] and the average error in CCT obtained in several test cases was found to be 0.0092s.

TABLE XVI: ACCURACY OF THE PROPOSED METHOD WITH EXCITER

Fault Location	Mode of separation	CCT with detailed model (time domain simulation) (s)	CCT (TEF) (s)	
			Classical Model	Detailed Model
29	Plant	0.132	0.081	0.121
15	Inter area	0.197	0.172	0.187

VIII. CONCLUSION

This paper proposes a novel technique to apply TEF method for assessment and alleviation of transient stability in real time. In the past, one of the reasons for not applying TEF method in real time was the computational difficulty associated with calculation of CUEP in real time. In this paper it is shown that a combination of BCU method (applied

offline) and the MOD technique (applied online) can ease the computational burden significantly, which enables possible application of the TEF method in a real-time.

A 10 generator and a 57 generator test system have been used to demonstrate the applicability of the proposed strategy. Both the offline data-base structure as well as the online computational results have been presented for both the systems. The impact of error in the measurement or prediction of the generator angles and speeds, on the energy margin have been analysed. A thorough audit of the computational burden of the proposed technique has also been presented which is essential for real-time application.

REFERENCE

- [1] N. Amjadi and S. F. Majedi, "Transient stability prediction by a hybrid intelligent system," *IEEE Trans. Power Syst.*, vol. 22, no. 3, pp. 1275-1283, August 2007.
- [2] T. Amraee and S. Ranjbar, "Transient Instability Prediction Using Decision Tree Technique," *IEEE Trans. Power Syst.*, Vol. 25, No. 3, pp. 3028-3037, 2013.
- [3] F. R. Gomez, A. D. Rajapakse, U. D. Annakkage and I. T. Fernando "Support vector machine based algorithm for post-fault transient stability status prediction using synchronized measurements," *IEEE Trans. Power Syst.*, vol. 26, no. 3, pp.1474-1483, 2011.
- [4] K. Mei and S. M. Rovnyak "Response-based decision trees to trigger one-shot stabilizing control," *IEEE Trans. Power Syst.*, vol. 19, no. 1, pp. 531 -537, 2004.
- [5] T. Athay, P. Podmore, and S. Virmani, "A practical method for the direct analysis of transient stability," *IEEE Trans. Power Apparatus and Systems*, vol. 98, no. 2, pp. 573-584, Mar. 1979.
- [6] A. A. Fouad, K. C. Kruempel, K. R. C. Mamandur, S. E. Stanton, M. A. Pai, and V. Vittal, "Transient Stability Margin as a Tool for Dynamic Security Assessment," *EPR Report EL-1755*, March, 1981.
- [7] A. A. Fouad, and S. E. Stanton, "Transient Stability of a Multimachine Power System. Part I: Investigation of the System Trajectory," *IEEE Trans. Power Apparatus and Systems*, vol. 100, pp. 4308-3424, 1981.
- [8] H. D. Chiang, F. Wu and P. Varaiya, "A BCU method for direct analysis of power system transient stability," *IEEE Trans. Power Syst.*, vol. 9, pp. 1194-1208, Aug. 1994.
- [9] N. Kakimoto, Y. Ohsawa and M. Hayashi, "Transient Stability Analysis of Multi-Machine Power Systems with Field Flux Decays Via Lyapunov's Direct Method," *IEEE Trans. Power Apparatus and Systems*, Vol. 99, No. 5, pp. 1819-1827, 1980.
- [10] T. Athay and D. I. Sun, "An Improved Energy Function for Transient Stability Analysis," *Proc. of International Symposium on Circuits and Systems*, Chicago, April 1981.
- [11] A. R. Bergen and D. J. Hill, "A Structure Preserving Model for Power System Stability Analysis," *IEEE Trans. Power Apparatus and Systems*, Vol. 100, pp. 25-35, Jan. 1981.
- [12] M. A. Pai, K. R. Padiyar and C. Radhukrishna, "Transient Stability Analysis of Multi-Machine AC/DC Power Systems Via Energy-Function Method," *IEEE PES Summer Meet.*, Portland, Oregon, 1981.
- [13] Y. Xue, Th. Van Cutsem, and M. R. Pavella, "A Simple Direct Method for Fast Transient Stability Assessment of Large Power System," *IEEE Trans. Power Syst.*, vol. 3, no. 2, may 1988.
- [14] A. A. Fouad, S. E. Stanton, "Transient Stability of a Multi-machine Power System. Part II: Critical Transient Energy," *IEEE Trans Power Apparatus and Systems*, Vol. 100, No. 7, July, 1981.
- [15] M. Takahashi, K. Matsuzawa, M. Sato, K. Omata, R. Tsukui, T. Nakamura, and S. Mizuguchi "Fast generation shedding equipment based on the observation of swings of generators," *IEEE Trans. Power Syst.*, vol.3, no.2, pp.439-446, 1988.
- [16] A. A. Fouad, A. Ghafurian , K. Nodehi and Y. Mansour, "Calculation of generation-shedding requirements of the B. C. Hydro system using transient energy function method", *IEEE Trans. Power Syst.*, vol. 1, no. 2, pp.17-24, 1986.
- [17] G. G. Karady and J. Gu, "A hybrid method for generator tripping," *IEEE Trans. Power Syst.*, vol. 17, no. 4, pp.1102 -1107, 2002.
- [18] G. Trudel, S. Bernard and G. Scott, "Hydro-Québec's defence plan against extreme contingencies," *IEEE Trans. Power Syst.*, vol. 8, no. 2, pp.445 -451, 1993.
- [19] H-C. Chang and H-C. Chen, "Fast Determination of Generation-Shedding in Transient Emergency State", *IEEE Trans Energy Conv.*, vol. PWRS8, pp.178-183, June 1993.
- [20] M. Djukanovic, D.J. Sobajic and Y.H. Pao, "Neural-Net Based Determination of Generator Shedding Requirements in Electric Power Systems", *IEE Proc.-C*, vol. 139, pp.427 -436 1992.
- [21] J. Geeganage, U. D. Annakkage, T. Weekes and B. A. Archer, "Application of Energy-Based Power System Features for Dynamic Security Assessment," *IEEE Trans. Power Syst.*, Vol. 30, No. 4, pp. 1957 - 196, July 2015.
- [22] N. Yorino et. al. "An Application of Critical Trajectory Method to BCU Problem for Transient Stability Studies," *IEEE Trans. Power Syst.*, Vol. 28, No. 4, pp. 4237 - 4244, 2013.
- [23] H. Ota, et.al., "Development of transient stability control system (TSC system) based on online stability calculation," *IEEE Trans on Power System*, Vol. PWRS11, No. 3, pp. 14631472, 1996.
- [24] A. A. Fouad and V. Vittal, "Power System Transient Stability Analysis Using the Transient Energy Function Method," Prentice Hall, New Jersey, 1992.
- [25] P. W. Sauer and M. A. Pai, "Power System Dynamics and Stability," Prentice Hall, New Jersey, 1998.
- [26] A. Llamas, J. De La Ree Lopez, L. Mili, A. G. Phadke and J. S. Thorp, "Clarifications on the BCU method for transient stability analysis," *IEEE Trans. Power Systems*, vol. 10, pp.210 -219, 1995.
- [27] N. Kakimoto, Y. Ohsawa, and M. Hayashi, "Transient Stability Analysis of Electric Power System Via Lure' Type Lyapunov Functions, Part I and II," *Trans. IEEE of Japan*, Vol. 98, No. 616, May/June, 1978.
- [28] P. Bhui and N. Senroy, "Online Identification of Tripped Line for Transient Stability Assessment," *IEEE Trans. Power Syst.*, vol. 31, no. 3, pp. 2214-2224, May 2016.
- [29] P. Bhui and N. Senroy, "Application of Recurrence Quantification Analysis to Power System Dynamic Studies," *IEEE Trans. Power Syst.*, vol. 31, no. 1, pp. 581-591, Jan. 2016.
- [30] A. A. Fouad , V. Vittal and O.. Taekyoo "Critical Energy For Transient Stability Assessment of A Multimachine Power System", *IEEE Trans.*, vol. PAS-103, pp.2199 -2206, 1984.
- [31] Y. Xue, and M. Pavella, "Critical-cluster identification in transient stability studies," *IET Gen. Trans. Distrib.*, Vol. 140, No. 6, pp. 481-489.
- [32] Friedman, J. H., J. Bentley, and A. R. Finkel, "An Algorithm for Finding Best Matches in Logarithmic Expected Time," *ACM Trans. Mathematical Software* 3, 209, 1977.
- [33] V. Chadalavada and V. Vittal, "Transient stability assessment for network topology changes: Application of energy margin analytical sensitivity", *IEEE Trans. Power Syst.*, vol. 9, no. 3, pp.1658 -1664, 1994.
- [34] [online], NRPG data, http://www.iitk.ac.in/eold/facilities/Research_labs/Power_System/NRPG-DATA.pdf, accessed 16 Oct 2015.
- [35] A. A. Fouad, V. Vittal, Y. X. Ni, H. R. Pota, K. Nodehi, H. Zein-Eldin, E. Vasahedi, and J. Kim, "Direct transient stability assessment with excitation control," *IEEE Trans. Power Syst.*, vol.4, no.1, pp.75-82, 1989.
- [36] G. Naresh, M. R. Raju, K. Ravindra, S. V. L. Narasimham. "Optimal Design of Multi-Machine Power System Stabilizer Using Genetic Algorithm," *Innovative Systems Design and Engineering*, vol. 2, No. 4.

Pratyasha Bhui received his M.Tech degree in Power and Energy System from Indian Institute of Technology Kharagpur, Kharagpur, India in 2013. He is currently pursuing PhD in the Dept. of Electrical Engineering in IIT Delhi, New Delhi, India. His research interests include power system dynamics, wide area measurement system.

Nilanjan Senroy (M'06) received the M.S. and Ph.D. degrees from Arizona State University, Tempe. He also has postdoctoral experience at the Center for Advanced Power Systems, Florida State University, Tallahassee. He is an Associate Professor in the Department of Electrical Engineering, Indian Institute of Technology, Delhi, India. His research interests include power system stability and control, signal processing and renewable energy